Photodegradation of Methylene Blue by Carbon Nanodots Synthesized from Olive Solid Wastes

Dr. Shadi Sawalha *, Hala Azzam , Rasha Bin Ali , Hanan Dweikat , Kayan Anaya

Chemical Engineering Department, An-Najah National University, Nablus, Palestine

**Corresponding author: sh.sawalha@najah.edu , +970599674156*

Abstract: Carbon Nanodots (CNDs) are emerging materials in the nanotechnology field as attractive photocatalysts, owing to their high water-solubility, good chemical and photostability, tunable photoluminescence and photoinduced phenomena.

This study aims to synthesize CNDs from olive solid wastes to be used as photocatalysts for the photodegradation of Methylene blue (M.B). CNDs were synthesized from olive solid waste by pyrolysis at 600 °C converted into carbonized material, followed by a chemical oxidation in the presence of hydrogen peroxide. The as-synthesized CNDs were utilized in this work as photocatalysts for the photodegradation of methylene blue at different conditions, such as; the catalyst concentration (dose), pH of the pollutant solution (M.B), salt content, light source distance, power of irradiation and pollutant concentration (M.B).

The degradation efficiency and rate were studied for all aforementioned factors, finding that the increase the CNDs dose into the M.B solution increases linearly both the efficiency and the rate. On the other hand, the maximum degradation rate was observed at pH = 10.6 with an efficiency of 92% after 120 minutes of irradiation. Moreover, the existence of NaCl salt in the pollutant solution affects adversely the degradation parameters showing a slight decrease in degradation rate, each 2 mg/ml addition decreased the rate with less than 1.2 folds. The potential and the distance of the visible light source from the pollutant cell have an obvious effect on the degradation, increasing the light power from 10 to 50 W, increased the degradation rate 16 times.

Keywords: Olive solid wastes, chemical oxidation, photodegradation, degradation efficiency and rate.

1. Introduction

Carbon Nanodots (CNDs) are small nano-sized carbon nano-materials less than 10 nm, were first synthesized in 2006 from carbon nanotubes (CNTs) during the process of electrophoresis[1], having internal sp^2 and external sp^3 carbon atoms[2]. CNDs surface is rich in hydrophilic functional groups, such as carboxyl, hydroxyl, epoxides, etc. which give them excellent and uniformly dispersion in polar solvents [3]. CNDs exhibit unique chemical and physical properties such as good luminescence, chemical inertness, low toxicity, excellent water solubility and conductivity [4]. They have been used for various applications, such as sensors, bio-imaging, electrogenerated chemiluminescence, solar to fuel production [5], and photocatalysts for pollutant/dye degradation [6].

CNDs are synthesized through two routes; top-down and bottom-up methods. They include pyrolytic decomposition or carbonization [7], chemical oxidation [8], arc discharge [9], laser etching [10], microwave [11] and hydrothermal or solvothermal methods [12].

CNDs have excellent photoluminescent properties in which they can convert visible light to a shorter wavelength that can extend the wide band-gap of a semiconductor [13]. CNDs are good for trapping and transferring electrons. Therefore, CNDs can be one of the best candidates in the photocatalytic degradation of organic dyes such as Methylene blue (M.B) [14]. Photocatalysis is an energy conversion process of semiconductor materials that can be initiated by light absorption. During photocatalysis, electrons and holes can be generated by light exposure [15]. CNDs can be considered to be good photocatalysts in the degradation of organic dyes owing to their strong visible-light absorption, excellent light-trapping ability, and high efficiency in the separation of photo-generated charge carriers[16].

The photodegradation of the pollutant in the presence of CNDs as photocatalysts is affected by several factors, which can play a role in obtaining the best degradation efficiency and higher rate. The most important factors are; concentration of photocatalyst [17], pH [18], salt concentrations [19], concentrations of pollutant [17], source of light and its location [20].

Synthetic organic dyes are commonly used in various industries, such as in textiles, leather, dyes, foods and cosmetics. They are one of the main water pollutants that can be a major threat to aquatic life [21,22].The most commonly used dye in textile industries is methylene blue, which is used for dyeing and cloth completion processes [14]. However, excessive exposure to methylene blue is harmful to human and aquatic life as it can cause skin allergies, dermatitis, nervous system disorders, and ultimately cardiovascular damages [23,24]. Therefore, it is important to search for economical and environmentally friendly methods to degrade and remove methylene blue and other dyes from pollutant waters.

In this work, CNDs synthesized from olive solid wastes as cheap and abundant precursor will be used as photocatalysts in order to remove organic pollutants such as methylene blue from water. Different factors that may affect the M.B photodegradation process will be studied. These factors are the photocatalyst dose, pH, pollutant concentration, source potential and location in addition to the salt content. Photodegradation efficiency and rate will be the most attractive parameters to be monitored

2. Materials and Methods

Olive solid wastes were obtained from an olive oil extraction plant in Nablus (Palestine). All required chemicals and reagents were purchased form Sigma-Aldrich and used without further purification. Distilled water was used in the synthesis and dialysis of carbon nanodots and also for preparing methylene blue solutions.

Steady state fluorescence spectra in an emission range of 350 to 650 nm and at different excitation wavelengths from 300 to 480 nm were conducted by using Perkin Elmer LS55 Fluorescence spectrophotometer. UV-Vis spectra were recorded on Thermo Scientific™ GENESYS 10S UV-Vis Spectrophotometer from 200 to 800 nm. Transmission Electron microscopy (TEM) analysis was performed by JEOL JEM 1400-Plus microscope operated at an accelerating voltage of 120 kV, equipped with GATAN US1000 CCD Camera. Samples were prepared by drop casting of CDs solution on Lacey carbon film coated copper TEM grids. Fourier transform infrared (FTIR) spectrum was recorded by a PerkinElmer Spectrum One instrument in the ATR (Attenuated Total Reflection) mode and 64 scans were acquired in the range of 4000–800 cm^{-1}. Z-potential measurements were carried out using a Malvern Nano ZS90 Zetasizer.

2.1 Synthesis of Carbon Nanodots (CNDs)

CNDs were synthesized according to the method published previously by the author and other co-workers [25]. Briefly, Olive solid wastes (OSWs) collected from Nablus were purified from impurities and residual oil by means of Soxhlet using hot water as solvent. Purified OSWs were dried and then pyrolyzed at 600°C to obtained a carbon-based material. After cooled down to room temperature a fine powder was prepared by using a pestle and mortar. 0.1 g of the carbon powder was dispersed in 10 ml deionized water contained 150 µl hydrogen peroxide (30 wt.%) and sonicated for 10 minutes. The mixture was then refluxed at 100°C for 90 min. To separate CNDs from large carbon particles, the mixture was centrifuged at 9900 rcf for 20 min., the resulted supernatant was the filtered through 0.2 µm microfilter and then dialyzed against distilled water through a dialysis membrane of 500 – 1000 Da cutoff. Obtained CNDs solution was stored in dark at 4°C for further use.

2.3 Photodegradation of Methylene Blue (M.B)

M.B solution with initial concentration of 35 µM was prepared by dissolving the weighed powder in appropriate volume of deionized water. UV-Vis spectrum scan was performed to M.B solution to find the wavelength of maximum absorption.

Firstly, 500 µl of 0.04 mg/ml CNDs solution were added to 3 ml of previously prepared M.B solution and left in dark for 2 hours to examine if CNDs will interact with M.B and behave as a catalyst.

3 ml of M.B solutions (35µM) in the absence and presence of CNDs were irradiated for 2 hours by visible light source of 50 W. The dose of the photocatalysts (CNDs) was altered by adding 200, 300, 400 and 500 µl of 0.04 mg/ml CNDs solution obtaining final concentrations of CNDs in M.B solution of 2.67, 4, 5.3, and 6.67 mg/L. (separate solutions were prepared). Before light irradiation, all solutions were left for half an hour to obtain an absorption-desorption equilibrium between solution species. The UV-Vis absorption was recorded for each sample at 668 nm (M.B

maximum absorption peak) with 10 minutes increment. The same irradiation procedures were carried out for all experiments.

Secondly, the effect of different parameters such as the pH, NaCl, light power/distance and pollutant (M.B) content on photodegradation process was examined at constant CNDs dose (6.67 mg/L). For the pH effect, different M.B solutions with pH of 3.8, 7, and 10.6 were prepared, the pH was adjusted by either drops of NaOH or HCl solutions. The effect of NaCl was followed after adding 6, 12 and 24 mg of salt into 3 ml M.B solution obtaining a final salt concentration of 2, 4, and 8 mg/ml respectively. Moreover, 10 and 50 W light sources were used and two distances of the light source (5 and 10 cm) form the M.B solution were also tested.

Finally, three pollutant (M.B) concentrations were prepared (35, 23 and 17.5 µM) and mixed with 500 µl of CNDs and then irradiated for 120 minutes to investigate the effect of M.B concentration on photodegradation process.

3. Results and Discussion

3.1 Synthesis and Characterizations of CNDs

Carbon nanodots were synthesized by a combination of bottom-up and top-down routes implementing the pyrolysis of olive solid waste at 600°C followed by extraction and chemical oxidation with H_2O_2 (Figure 1). H_2O_2 acts as a strong oxidizing agent helping in breaking down the carbonaceous particles present in pyrolyzed olive solid wastes, producing CNDs rich of oxygenated groups on their surfaces [26].

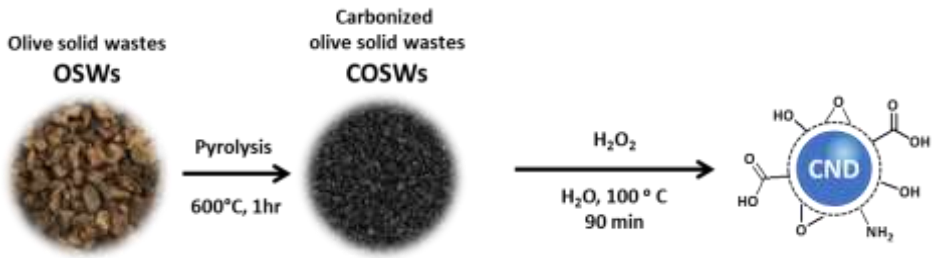

Figure 1: Synthesis procedure of CNDs

The morphology of synthesized CNDs was investigated by using the Transmission Electron Microscope (TEM). The TEM micrograph shows well dispersed nanoparticles with good contrast and narrow size dispersion from 1-4 nm with average size of (2.8±0.6 nm). The TEM micrograph and size distribution histograms are illustrated in Figure 2(a).

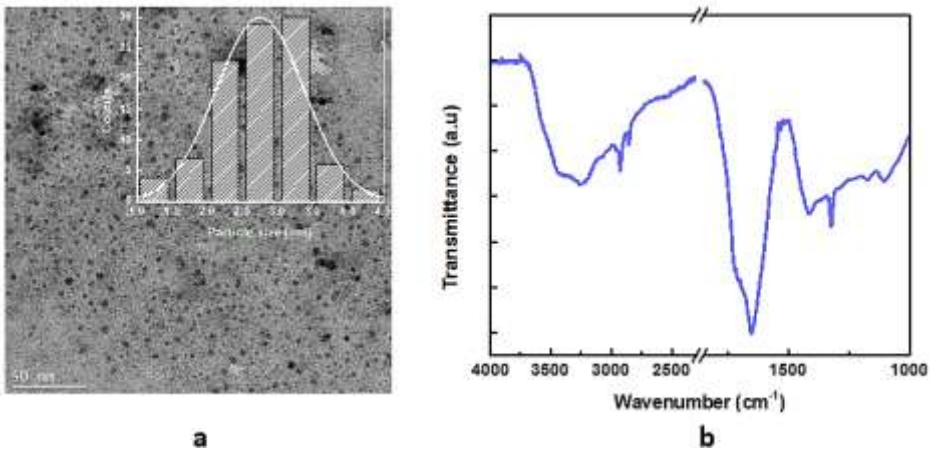

Figure 2: (a) TEM Micrograph, size distribution histogram (the inset). (b) FT-IR spectrum of synthesized CNDs.

The surface functional groups of prepared CNDs were acquired using FT-IR. The FT-IR spectrum in Figure 2(b) shows different peaks at 3424, 3236, 2923/2850, 1656, 1412, 1320, 1116 and 1096 cm^{-1}. These peaks are attributed to –OH, N-H, C-H, C=O (carbonyl), COO- (carboxylate), C-OH (hydroxyl) and C-O-C (epoxide) respectively [27,28]. The presence of oxidized and acidic groups on the surface leads to a strong negative charge of -32 eV (*@10 mM P.B. (pH =7.4))* and -18 eV *@ pH = 3* theses values were attained by ζ-potentials measurements [29-31]. Such negative potential value confers to the excellent solubility of CNDs in water [32].

The optical properties of synthesized CNDs were explored by conducting the UV-Vis absorption and photoluminescence measurements. Usually, the absorption spectrum of CNDs appears in the UV region and the tail extending towards the visible region. UV-visible spectrum of CNDs as in Figure 3(a) shows a strong absorption at 220 – 320 nm which can be related to the π-π^* and n-π^* transition arising from aromatic C=C bonds (sp^2 domain) and C=O groups respectively [31,33].

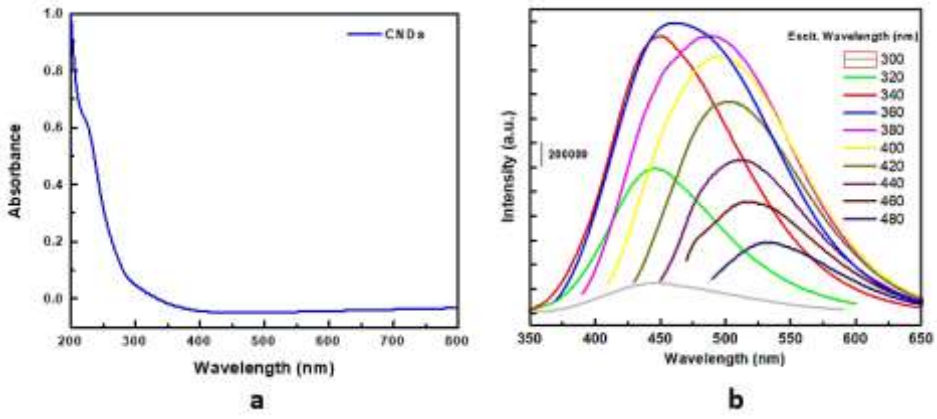

Figure 3: (a) UV-Vis Spectrum of CNDs, (b) Photoluminescence emission at different excitation wavelengths.

Furthermore, detailed photoluminescence (PL) measurement for CNDs (Figure 3(b)) was carried out at different excitation wavelengths. The fluorescence spectra of CNDs show a maximum emission at 460 nm (Ex.360 nm). The emission is excitation dependent, showing peak shifts from 440 to 540 nm while the excitation wavelength changes from 300 to 480 nm, this behavior is a well-known phenomenon of most carbon nanodots [34-36].

3.2 Photodegradation of Methylene Blue

The methylene blue solution showed a maximum UV-Vis absorption at 668 nm. To test whether CNDs will act as catalysts or photocatalysts, equal amounts (500µl) of CNDs (0.04 mg/ml) were spiked into M.B solutions, one of them was left in dark and the other was irradiated for 120 min. Every 10-15 minutes the UV-Vis absorption at 668 nm was recorded as shown in Figure 4(a) and the degradation efficiency was evaluated and plotted versus time (Figure 4(b)).

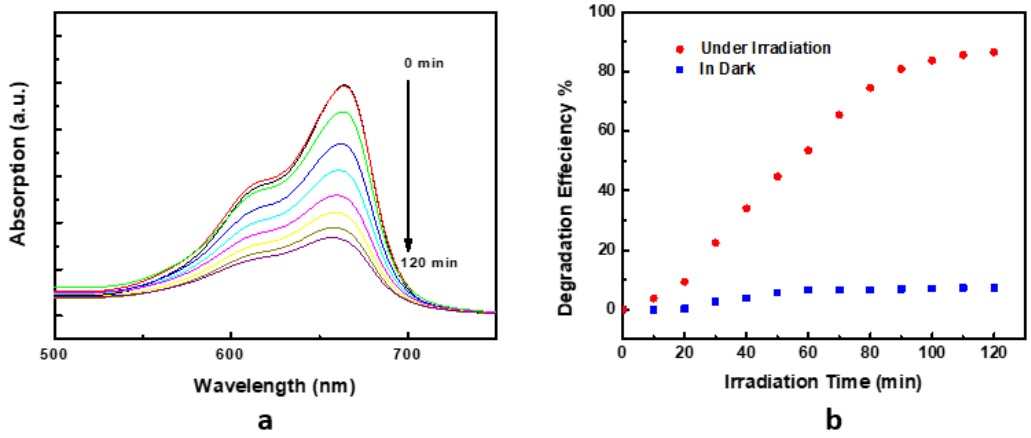

Figure 4: (a) UV-Vis absorption of M.B solution spiked with 500 µl of CNDs and irradiated by 50 W visible light for 120 minutes, (b) The degradation efficiency of M.B under light irradiation and in dark.

It is evident from figure 4(b) that CNDs behave as photocatalysts not as catalysts because they have worked only under irradiation without any significant effect on the concentration of M.B when the mixture remained in dark.

Several factors affect the degradation process (degradation efficiency and rate) of the Methylene blue as follows.

3.2.1 Effect of Dose of Photocatalyst on Degradation of M.B.

The degradation of methylene blue in the presence of different amounts of CNDs was investigated, the concentration of the CNDs (Dose) was changed. 0, 2.67, 4, 5.3, and 6.67 mg/L concentrations of CNDs in M.B solutions were irradiated for 120 minutes, the UV-Vis absorptions were recorded at 668 nm and the degradation efficiency at different time was estimated for each photocatalyst concentration and illustrated in Figure 5(a). As shown in the Figure the degradation efficiency at 120 min is increased from 27.4% in the absence of the photocatalyst up to 86.5% in the

presence of CNDs with 6.67 mg/L. It is also obvious in Figure 5(b) the difference in M.B solution color in the presence and absence of CNDs. There was no degradation of the MB dye in the dark because it is a heterocyclic aromatic chemical compound that contains three combined aromatic rings with (C–S), (CN) and (CN = —) functional groups. Due to the complicated carbon-bonding in the MB structure, the adsorption reaction of CNDs and M.B molecules was difficult [20]. While the slow degradation of M.B in the absence of photocatalyst (27.4%) could be ascribed to the to the lone pairs that are located at nitrogen and sulfur atoms in the M.B structure. These are electron-rich regions, which became active once they were irradiated. They exhibited repulsion forces between bond pair electrons, leading to instability, and hence, they attacked the associated water molecules to form a stable bond [37].

The degradation efficiency was calculated according the following equation:

$$Degradation\ Effeciency\ (\%D) = \frac{A_0 - A}{A_0} \times 100\% \qquad (1)$$

Where A_0 the absorbance of M.B at time zero, A absorbance at time = t

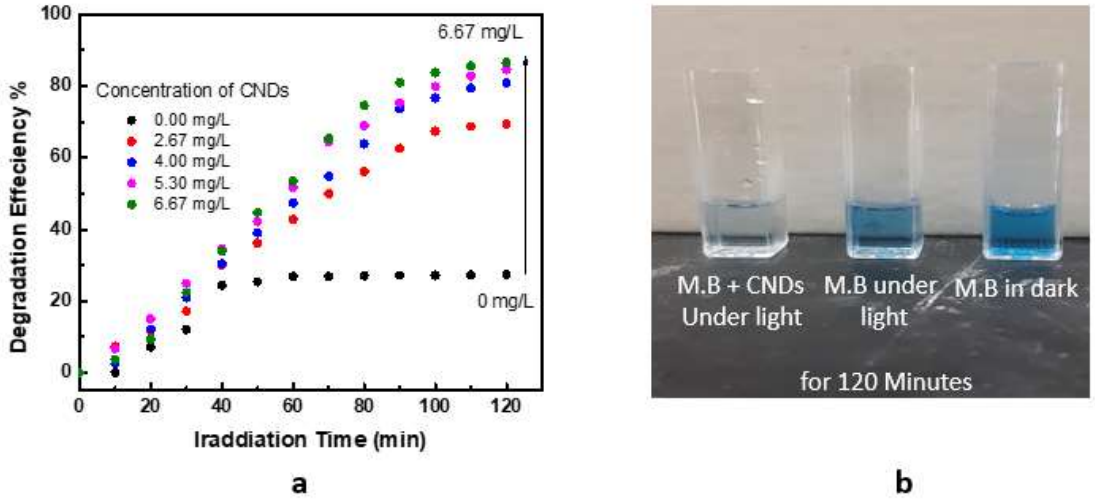

Figure 5: (a) Photodegradation rate of M.B at different concentration of CNDs (dose), (b) Degradation of M.B (color change) in dark and under irradiation in the absence of CNDs and under light irradiation in the presence of CNDs

Another important degradation parameter that should be estimated is the degradation rate. Herein, we have suggested Langmuir–Hinshelwood dynamic model [20], where the degradation kinetics of M.B could be simplified according to the pseudo first-order kinetic as shown in equation (2)

$$\ln\left(\frac{\mathrm{Co}}{\mathrm{C}}\right) = \mathrm{k} \times \mathrm{t} \qquad (2)$$

Where C_0 and C should be the equilibrium concentration of M.B and the concentration of M.B after irradiation time t, respectively. C_0 and C are equivalent to the absorbance of the dyes at time

zero (A_0) and the absorbance of the dyes after degradation time *t* (*A*), respectively and *k* represents the dye degradation rate constant.

Therefore, a fitted plot of $ln(A_0/A)$ versus time leads to a straight line with a slope representing the degradation rate as in Figure 6 (a). The degradation rate for all doses (0 to 0.667 mg/L CNDs) was estimated and illustrated in Figure 6 (b)

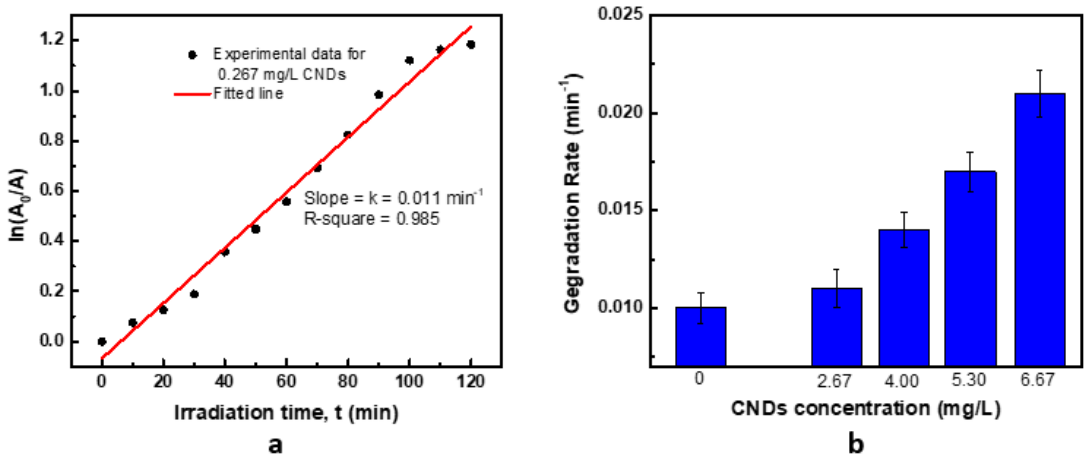

Figure 6: (a) Fitting of Langmuir–Hinshelwood dynamic model at 2.67 mg/L CNDs, (b) Degradation rate of M.B at different concentration of CNDs

Figure 6(b) shows clearly the effect of the photocatalyst dose (CNDs) on the degradation of M.B solution with an increase of about 150% in the degradation rate when the dose concentration increases from 2.67 to 6.67 mg/L. This significant increase could be ascribed to the increase in the active sites (photocatalyst) in the solution and the ability to convert rapidly the M.B into harmless products such as CO_2 and H_2O. Moreover, the degradation mechanism would be explained by Figure 7. When photons of appropriate energy excite CNDs, electrons were excited from the ground state (valence band) to excitation state (conduction band), generating excess electrons (e−) and holes (h+). Due to the rich presence of surface defects on CNDs, some of the excited carriers are trapped, and the recombination of e- and h+ are hindered. As a result, the methylene blue could be oxidized by the h+ directly to cause the degradation [38]. In the meantime, some of the e− could be captured by oxygen dissolved in the solution, forming super oxide radicals, some of the h+ could interact with surface-adsorbed H_2O to form hydroxyl radicals. Reactive oxygen species (ROS) , super oxide [39] and hydroxyl radical [38,40]are known to degrade organic dyes.

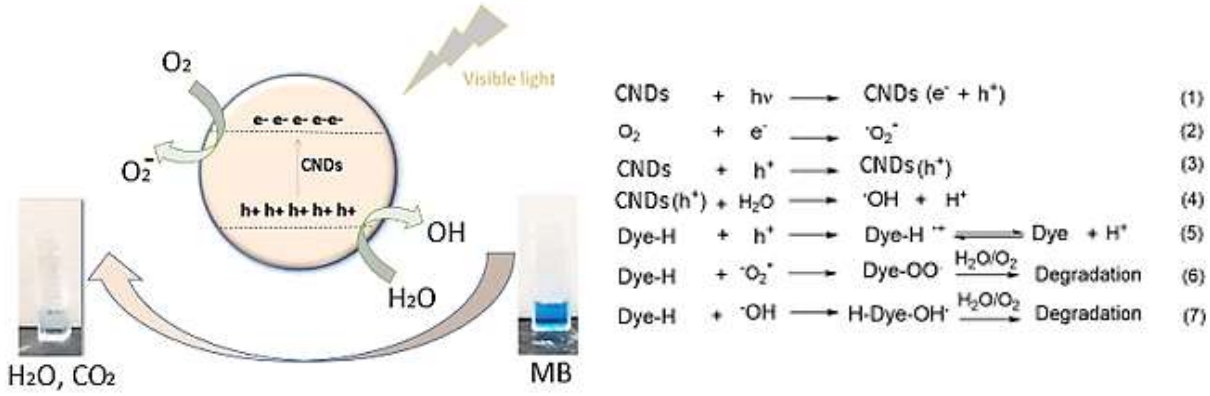

Figure 7: Mechanism of Methylene Blue Degradation

3.2.2 Effect of pH on Degradation of M.B

In general, pH was considered to be a critical role during the photocatalytic process. It impacts the surface charges of photocatalysts, electrostatic interactions between the pollutants and the photocatalysts, the formation of pollutant and the ionization states of M.B [41].

The degradation efficiency and rate of M.B were increased dramatically when the pH of the solution increased from 3.8 to 10.6, the degradation efficiency has been increased from about 64% to 92%, while the rate increased from 0.0012 to 0.061 min^{-1}. See Figure 8 (a) and (b). This could be ascribed to the increase in negativity (anionic) of CNDs, as Zeta-potential decreased from -18 eV at pH=3 (acid condition) to -32 eV on pH =7.4, this change in negativity could be related to increase in hydroxyl surface groups which in their turn act as surface traps causing more hindering of e- and h+ recombination [20].

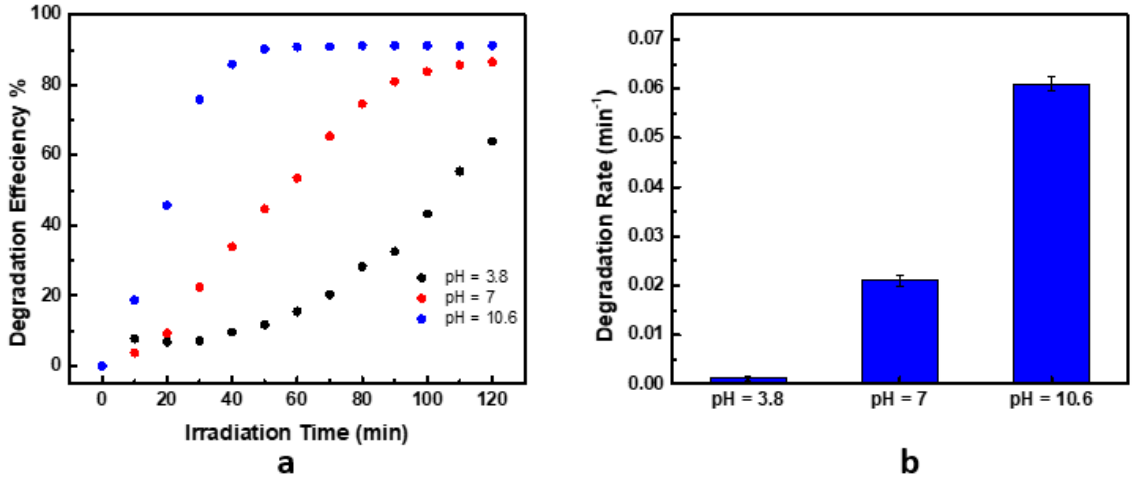

Figure 8: Effect of pH on the degradation of M.B. (a) Degradation efficiency, (b) Degradation rate

3.2.3 Effect of Salt on Photodegradation of M.B

Sodium chloride was added to the pollutant solution (M.B) to explore its influence on the degradation process. Figure 9 displays the degradation rate of M.B under four different concentrations of NaCl salt (0, 2, 4, and 8 mg/ml).

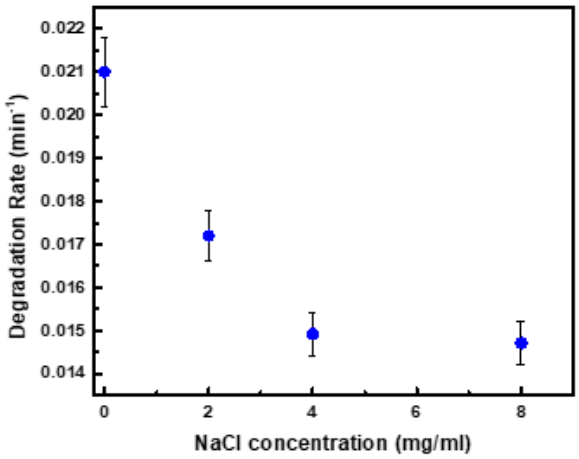

Figure 9: Degradation rate of M.B at different concentrations of NaCl

Figure 9 shows a decrease in degradation rate with increase in NaCl concentration, this could be related to that NaCl salt behaves as a suppressing agent impedes slightly the generation of e- and h+ after excitation from the ground state [19].

3.2.4 Effect of the distance of light source on M.B photodegradation

The distance of the light source from the pollutant was changed from 10 cm to 5 cm, this proximity causes an improvement in degradation efficiency and also a slight increase in degradation rate from 0.02067 to 0.02435 1/min (see Figure 10). The closeness of light results in much more incident photons onto CNDs surface, causing more or fast generation of holes and electrons upon excitation.

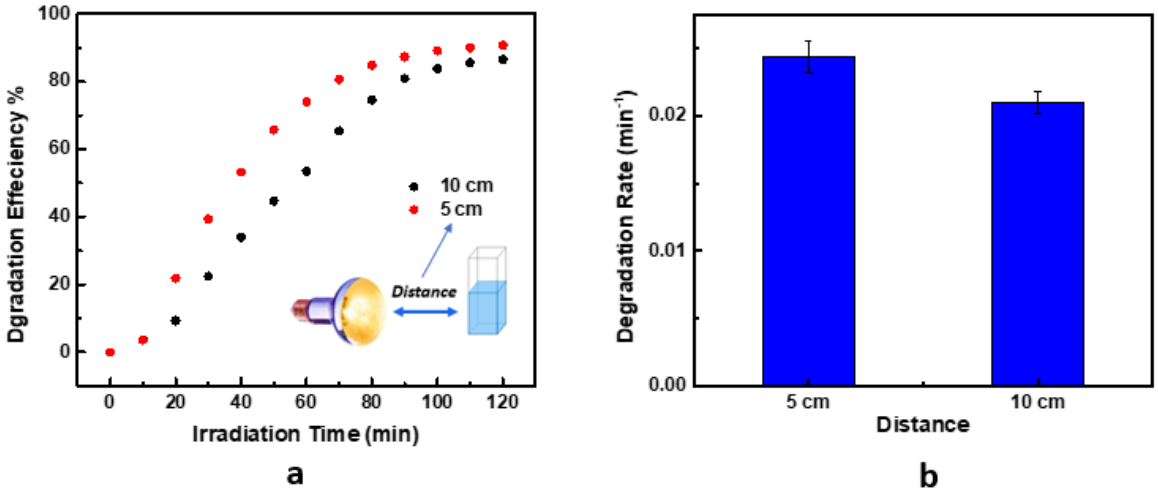

Figure 10: Effect of light source's distance on degradation efficiency and rate of M.B

3.2.5 Effect of the power of light source on M.B photodegradation

Photocatalytic phenomena rely on the energy supplied by light quanta. Electron–hole pairs are generated in the conduction band and valance band of a photocatalytic material when they receive photons with energy equal to or greater than its band gap [42]. Therefore, the light intensity plays a critical role in photocatalytic dye removal. The visible yellow light with powers 50 and 10 watt were applied. Figure 11 shows the degradation efficiency at both powers. It is obvious that the power of 10 W is not sufficient to cause a significant degradation of M.B. due to very low number of emitted photons which leads to very low degradation efficiency and rate; 16% (@ 120 minutes and 0.0012 min^{-1} respectively.

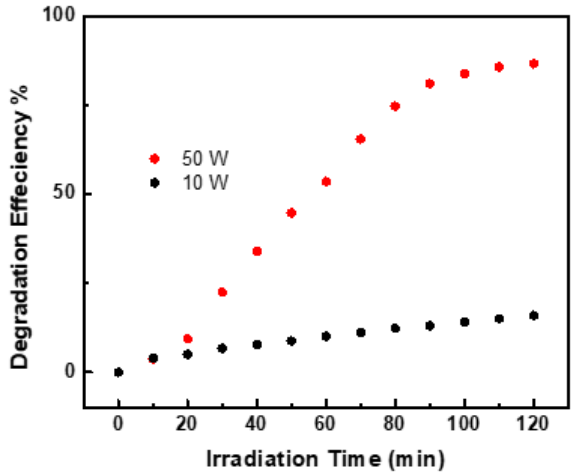

Figure 11: Degradation efficiency of M.B at different light source powers

3.2.6 Effect of the initial concentration of M.B on its biodegradation

Three concentrations of M.B (35, 23.33, 17.5) µM were spiked with same amounts of CNDs and irradiated for 120 minutes. Figure 12 illustrates the degradation efficiency and rate of M.B at these concentrations. The degradation efficiency remains nearly constant while the degradation rate decreased with increasing the concentration. Because photodegradation occurs due to light absorbed by CNDs, therefore, this decrease could be ascribed to that excessive M.B may hamper the reception of light onto the CNDs surface and delay or hinder the activation of the photocatalytic processes [43].

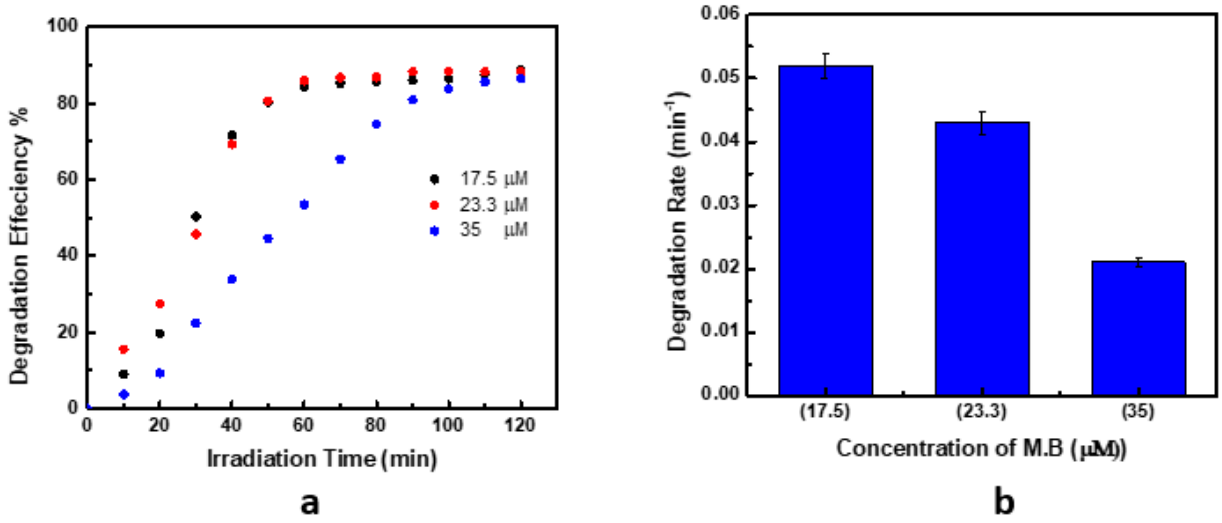

Figure 12: Degradation of different concentrations of M.B: (a) Degradation efficiency, (b) Degradation rate.

It is worthy to point that CNDs prepared in this work are shown to be very promising candidates for dye photodegradation, environment protection, and cleanliness. Synthesized CNDs have been compared with other works in terms of M.B photodegradation efficiency and rate showing excellent results. For instance, a degradation efficiency of 86-92%/120 min and a rate of 0.021 (pH = 7) and 0.061 min^{-1}(pH = 10.6) were obtained for a dose of carbon dots equal to 6.66 mg/L which could be considered attractive and important results of a photocatalyst when they compared to C-dots synthesized from citric acid, there, the photocatalyst resulted in degradation efficiency and rate of 99.9%/170 min and 0.024 min^{-1} respectively with a dose of 750 mg/L CNDs [44].

4. Conclusion

An efficient visible-light photocatalyst CNDs was facilely prepared by combination of bottom-up and top-down routes using pyrolysis and chemical oxidation methods. The synthesized CNDs was fluorescent with about 3 nm size. The photocatalytic activity of these dots was monitored through the degradation of methylene blue dye after irradiation of yellow visible light for 120 minutes. Degradation efficiency and rate were estimated for different conditions, finding that the dose of the photocatalyst (CNDs) in the dye solution had a great effect on both efficiency and rate with maximum efficiency and rate of 87% and 0.021 min^{-1} respectively when a dose of 6.67 mg/L was used. pH of the solution showed a significant enhancement of the photodegradation process, for instance, at pH = 10.6 the degradation rate was the highest value (0.061 min^{-1}) with an efficiency of 92% after 120 minutes. Moreover, it was concluded that an increase in salt content affects adversely the degradation rate and the same results were obtained in the case of increasing the pollutant concentration but with different decrease ratios. Finally, it was found that the power of the source and position with respect to the targeted pollutant have noticeable effect on the degradation process, an increase in degradation rate was obtained for high power and low distances.

Funding: "This research received no external funding"

Acknowledgment: Authors would like to thank prof. Prato's group at CIC biomaGUNE in Sansebastian-Spain and Prof. Valli's group at University of Salento- Italy for their technical help and support in conducting some analytical tests such the transmission electron microscope (TEM).

References

1. Xu X, Ray R, Gu Y *et al.* Electrophoretic Analysis and Purification of Fluorescent Single-Walled Carbon Nanotube Fragments. *Journal of the American Chemical Society*, (2004), 126(40), 12736-12737.
2. Cheng Y, Bai M, Su J *et al.* Synthesis of fluorescent carbon quantum dots from aqua mesophase pitch and their photocatalytic degradation activity of organic dyes. *Journal of Materials Science & Technology*, (2019), 35(8), 1515-1522.
3. Yadav A, Bai L, Yang Y *et al.* Lasing behavior of surface functionalized carbon quantum dot/RhB composites. *Nanoscale*, (2017), 9(16), 5049-5054.
4. Das R, Bandyopadhyay R, Pramanik P. Carbon quantum dots from natural resource: A review. *Materials Today Chemistry*, (2018), 8, 96-109.
5. Namdari P, Negahdari B, Eatemadi A. Synthesis, properties and biomedical applications of carbon-based quantum dots: An updated review. *Biomedicine & Pharmacotherapy*, (2017), 87, 209-222.
6. Di J, Xia J, Ge Y *et al.* Novel visible-light-driven CQDs/Bi2WO6 hybrid materials with enhanced photocatalytic activity toward organic pollutants degradation and mechanism insight. *Applied Catalysis B: Environmental*, (2015), 168-169, 51-61.
7. Zhang X, Jiang M, Niu N *et al.* Natural-Product-Derived Carbon Dots: From Natural Products to Functional Materials. *ChemSusChem*, (2018), 11(1), 11-24.
8. Miao P, Han K, Tang Y, Wang B, Lin T, Cheng W. Recent advances in carbon nanodots: synthesis, properties and biomedical applications. *Nanoscale*, (2015), 7(5), 1586-1595.
9. Dey S, Govindaraj A, Biswas K, Rao CNR. Luminescence properties of boron and nitrogen doped graphene quantum dots prepared from arc-discharge-generated doped graphene samples. *Chemical Physics Letters*, (2014), 595-596, 203-208.
10. Cao L, Wang X, Meziani MJ *et al.* Carbon Dots for Multiphoton Bioimaging. *Journal of the American Chemical Society*, (2007), 129(37), 11318-11319.
11. Li H, Kang Z, Liu Y, Lee S-T. Carbon nanodots: synthesis, properties and applications. *Journal of Materials Chemistry*, (2012), 22(46), 24230-24253.
12. Sahu S, Behera B, Maiti TK, Mohapatra S. Simple one-step synthesis of highly luminescent carbon dots from orange juice: application as excellent bio-imaging agents. *Chemical Communications*, (2012), 48(70), 8835-8837.
13. Rani UA, Ng LY, Ng CY, Mahmoudi E. A review of carbon quantum dots and their applications in wastewater treatment. *Advances in Colloid and Interface Science*, (2020), 278, 102124.
14. Rani UA, Ng LY, Ng CY, Mahmoudi E, Ng Y-S, Mohammad AW. Sustainable production of nitrogen-doped carbon quantum dots for photocatalytic degradation of methylene blue and malachite green. *Journal of Water Process Engineering*, (2021), 40, 101816.

15. Zhou C, Zeng G, Huang D *et al.* Distorted polymeric carbon nitride via carriers transfer bridges with superior photocatalytic activity for organic pollutants oxidation and hydrogen production under visible light. *Journal of Hazardous Materials*, (2020), 386, 121947.
16. Abd Rani U, Ng LY, Ng CY, Mahmoudi E, Ng Y-S, Mohammad AW. Sustainable production of nitrogen-doped carbon quantum dots for photocatalytic degradation of methylene blue and malachite green. *Journal of Water Process Engineering*, (2021), 40, 101816.
17. Lu Q, Zhang Y, Liu S. Graphene quantum dots enhanced photocatalytic activity of zinc porphyrin toward the degradation of methylene blue under visible-light irradiation. *Journal of Materials Chemistry A*, (2015), 3(16), 8552-8558.
18. Wang F, Wu Y, Wang Y *et al.* Construction of novel Z-scheme nitrogen-doped carbon dots/{0 0 1} TiO2 nanosheet photocatalysts for broad-spectrum-driven diclofenac degradation: Mechanism insight, products and effects of natural water matrices. *Chemical Engineering Journal*, (2019), 356, 857-868.
19. Yu H, Huang J, Jiang L *et al.* Enhanced photocatalytic tetracycline degradation using N-CQDs/OV-BiOBr composites: Unraveling the complementary effects between N-CQDs and oxygen vacancy. *Chemical Engineering Journal*, (2020), 402, 126187.
20. Jiang R, Lu G, Yan Z, Wu D, Zhou R, Bao X. Insights into a CQD-SnNb2O6/BiOCl Z-scheme system for the degradation of benzocaine: Influence factors, intermediate toxicity and photocatalytic mechanism. *Chemical Engineering Journal*, (2019), 374, 79-90.
21. Desa AL, Hairom NHH, Ng LY, Ng CY, Ahmad MK, Mohammad AW. Industrial textile wastewater treatment via membrane photocatalytic reactor (MPR) in the presence of ZnO-PEG nanoparticles and tight ultrafiltration. *Journal of Water Process Engineering*, (2019), 31, 100872.
22. Ong CB, Mohammad AW, Ng LY. Integrated adsorption-solar photocatalytic membrane reactor for degradation of hazardous Congo red using Fe-doped ZnO and Fe-doped ZnO/rGO nanocomposites. *Environmental Science and Pollution Research*, (2019), 26(33), 33856-33869.
23. Abdulla NK, Siddiqui SI, Tara N, Hashmi AA, Chaudhry SA. Psidium guajava leave-based magnetic nanocomposite γ-Fe2O3@GL: A green technology for methylene blue removal from water. *Journal of Environmental Chemical Engineering*, (2019), 7(6), 103423.
24. Üner O. Hydrogen storage capacity and methylene blue adsorption performance of activated carbon produced from Arundo donax. *Materials Chemistry and Physics*, (2019), 237, 121858.
25. Sawalha S, Silvestri A, Criado A, Bettini S, Prato M, Valli L. Tailoring the sensing abilities of carbon nanodots obtained from olive solid wastes. *Carbon*, (2020), 167, 696-708.
26. Liu QR, Zhang JJ, He H *et al.* Green Preparation of High Yield Fluorescent Graphene Quantum Dots from Coal-Tar-Pitch by Mild Oxidation. *Nanomaterials-Basel*, (2018), 8(10), 844-854
27. Das P, Bose M, Ganguly S *et al.* Green approach to photoluminescent carbon dots for imaging of gram-negative bacteria Escherichia coli. *Nanotechnology*, (2017), 28(19), 195501-1955014
28. Radhakrishnan K, Panneerselvam P, Marieeswaran M. A green synthetic route for the surface-passivation of carbon dots as an effective multifunctional fluorescent sensor for the recognition and detection of toxic metal ions from aqueous solution. *Anal Methods-Uk*, (2019), 11(4), 490-506.
29. Bandi R, Gangapuram BR, Dadigala R, Eslavath R, Singh SS, Guttena V. Facile and green synthesis of fluorescent carbon dots from onion waste and their potential applications as sensor and multicolour imaging agents. *Rsc Adv*, (2016), 6(34), 28633-28639.

30. Bettini S, Sawalha S, Carbone L, Giancane G, Prato M, Valli L. Carbon nanodot-based heterostructures for improving the charge separation and the photocurrent generation. *Nanoscale*, (2019), 11(15), 7414-7423.
31. Patidar R, Rebary B, Sanghani DA, Bhadu GR, Paul P. Fluorescent carbon nanoparticles obtained from charcoal via green methods and their application for sensing Fe3+ in an aqueous medium. *Luminescence*, (2017), 32(8), 1466-1472.
32. Xue MY, Zhan ZH, Zou MB, Zhang LL, Zhao SL. Green synthesis of stable and biocompatible fluorescent carbon dots from peanut shells for multicolor living cell imaging. *New J Chem*, (2016), 40(2), 1698-1703.
33. Ghosh S, Satapathy SS, Ghosh K, Jauhari S, Panda SK, Si S. Carbon Dots Assisted Synthesis of Gold Nanoparticles and Their Catalytic Activity in 4-Nitrophenol Reduction. *Chemistryselect*, (2019), 4(12), 3416-3422.
34. Zhu SJ, Song YB, Zhao XH, Shao JR, Zhang JH, Yang B. The photoluminescence mechanism in carbon dots (graphene quantum dots, carbon nanodots, and polymer dots): current state and future perspective. *Nano Res*, (2015), 8(2), 355-381.
35. Arcudi F, Dordevic L, Prato M. Synthesis, Separation, and Characterization of Small and Highly Fluorescent Nitrogen-Doped Carbon NanoDots. *Angew Chem Int Edit*, (2016), 55(6), 2107-2112.
36. Sharma A, Gadly T, Gupta A, Ballal A, Ghosh SK, Kumbhakar M. Origin of Excitation Dependent Fluorescence in Carbon Nanodots. *J Phys Chem Lett*, (2016), 7(18), 3695-3702.
37. Ok KM, Ohishi Y, Mitazono Y, Muta H, Kurosaki K, Yamanaka S. Bi-doped lanthanum molybdate: Enhancing the anharmonicity and reducing the thermal conductivity using Bi3+ with lone pair electrons. *Ceramics International*, (2018), 44(13), 15833-15838.
38. Das GS, Shim JP, Bhatnagar A, Tripathi KM, Kim T. Biomass-derived carbon quantum dots for visible-light-induced photocatalysis and label-free detection of Fe (III) and ascorbic acid. *Scientific reports*, (2019), 9(1), 1-9.
39. Zhou Y, Zahran EM, Quiroga BA *et al.* Size-dependent photocatalytic activity of carbon dots with surface-state determined photoluminescence. *Applied Catalysis B: Environmental*, (2019), 248, 157-166.
40. Hu S, Tian R, Dong Y, Yang J, Liu J, Chang Q. Modulation and effects of surface groups on photoluminescence and photocatalytic activity of carbon dots. *Nanoscale*, (2013), 5(23), 11665-11671.
41. Lin X, Liu C, Wang J, Yang S, Shi J, Hong Y. Graphitic carbon nitride quantum dots and nitrogen-doped carbon quantum dots co-decorated with BiVO4 microspheres: A ternary heterostructure photocatalyst for water purification. *Separation and Purification Technology*, (2019), 226, 117-127.
42. Anwer H, Mahmood A, Lee J, Kim K-H, Park J-W, Yip ACK. Photocatalysts for degradation of dyes in industrial effluents: Opportunities and challenges. *Nano Research*, (2019), 12(5), 955-972.
43. Chen J, Shu J, Anqi Z, Juyuan H, Yan Z, Chen J. Synthesis of carbon quantum dots/TiO2 nanocomposite for photo-degradation of Rhodamine B and cefradine. *Diamond and Related Materials*, (2016), 70, 137-144.
44. Peng Z, Zhou Y, Ji C *et al.* Facile Synthesis of "Boron-Doped" Carbon Dots and Their Application in Visible-Light-Driven Photocatalytic Degradation of Organic Dyes. *Nanomaterials (Basel)*, (2020), 10(8), 1560.